

Is it appropriate to apply Hertz model to describe cardiac myocytes' mechanical properties by atomic force microscopy nanoindentation?

A.A. Soufivand¹, M. Navidbakhsh¹, M. Soleimani²

¹Biomechanics Group, School of Mechanical Engineering, Iran University of Science and Technology (IUST), Narmak, Tehran, Iran

²Hematology Group, School of Medical Science, Tarbiat Modares University, AmirAbad Street, Tehran, Iran
E-mail: anahita.a.soufivand@gmail.com

Published in Micro & Nano Letters; Received on 11th January 2014; Accepted on 14th February 2014

An analysis is conducted of application of the Hertz model for measuring the cardiac myocytes' mechanical properties. Atomic force microscopy (AFM) was used, which characterises the cellular mechanical properties at a nanoscale precision. The Hertz model, the most common model in contact mechanics, was applied to the experimental data and an elastic modulus was determined by analysing the relationship between the AFM indentation force and the depth. To determine the Hertz model appropriateness accurately, the contribution of the viscous properties, the cell adherence and the elastic modulus extracting method were examined. The elastic moduli were 48.08 ± 2.26 kPa and 55.67 ± 2.56 kPa, respectively, with two different evaluation approaches. The cardiac myocyte exhibited a nonlinear elastic behaviour since the elastic modulus determined by the Hertz model was not constant in the different indentation depths. Furthermore, the viscous dissipation was negligible; therefore the mechanical behaviour of this cell type can be well described by appropriate hyperelastic models.

1. Introduction: The mechanical properties of the cells play a key role in determining the changes during the essential functions such as contraction, crawling and migration. The contracting cardiac muscle cells have particular cytoskeletal arrangements to accommodate the specialised role they play in heart tissue. In the experimental cell mechanics studies, these cells are isolated from the heart ventricles [1]. The ventricular cardiac wall strains display significant temporal, regional and transmural variations [2]. The constitutive properties of the myocardium are three-dimensional, anisotropic, nonlinear and time dependent [3]. A straightforward method of heart tissue modelling is to calculate the active mechanical properties obtained from a cellular model [4]. It is applicable in determining the end-diastolic tension in open heart surgery. After performing a cardiac surgical operation, a surgeon needs a functional value of pressure to set into the heart which depends on the end-diastolic tension [5].

Recent advances in the micro and the nano technologies have enabled the development of new experimental and modelling approaches to study the cell biomechanics that were not possible previously [6]. Many single-cell measurement tools have been developed over the last few decades to quantify the cellular responses under mechanical force/deformation such as atomic force microscopy (AFM), micropipette aspiration, magnetic twisting cytometry and so on [7, 8]. AFM-nanoindentation, one of the most powerful tools, has been recently used to analyse the mechanical properties changes in the cardiac myocytes [9]. It allows one to obtain the topographical images and to probe the mechanical properties of the living cells [10–14].

By indenting the cell surface with the tip of the cantilever and measuring the force at each indentation depth, the cell mechanics are probed. The mechanical properties of the sample are usually estimated by fitting the obtained experimental data with a suitable contact model. For the cells subjected to the conventional mechanical modes of loading, various models have been developed and applied [15, 16]. For the cardiomyocyte, there are several models coupled with the mechanical properties of the cell such as the mechano-chemical models [17]. However, in this Letter, only the mechanical properties of the cardiomyocyte were extracted. In the AFM-nanoindentation, Hertz's theory is the most common

approach to analysing the contact mechanics. This approach is based on infinitesimal strains and a linear elasticity and assumes that the axisymmetric, the isotropic and the semi-infinite bodies are in contact with each other, which was applied in the cardiomyocytes mechanics studies [18, 19].

The aim of the work reported in this Letter was to examine the Hertz contact model and to assess the suitability of this model for probing the mechanical properties of the cardiac contracting cells. AFM was used and to accurately determine the Hertz model's suitability we examined the cell adherence, the hysteresis effect, the elastic modulus calculation manner and the effect of the probe tip shape.

2. Materials and methods

2.1. Preparing cells: The cardiac myocytes were prepared in the laboratory of the Tarbiat Modarres University hematology group (North Amir Abad Street, Tehran, Iran), from 13 to 15 days embryonic mouse hearts which were born from 8 to 12 weeks white NMRI mice (provided by the RAZI institute, Tehran, Iran). The embryonic heart was cut into small parts in the Dulbecco's modified eagle medium (DMEM) containing a 10% fetal calf serum (FCS). They were flushed and the separated cells were washed for eliminating the unwanted cells. Then, these cells were put in 10 cm diameter medium plates containing the DMEM with a 2% FCS and were placed for 24 h in an incubator in a wet 37°C environment with 5% CO₂. After 24 h, live ventricle heart cells were attached to the container floor and the other cells were suspended and they were thrown away. The myocytes were kept in a CO₂ incubator for six to seven days. In this time, each two days, their medium was changed and they filled the whole container floor. By using 0.25% trypsin and 0.02% edetic acid (EDTA), the cells were detached from the plate floor and effect of trypsin was neutralised by the FCS. These cells were centrifuged for 3 min with 1200 rpm in sterilised 15 ml conical tubes. Then, fresh DMEM with a 2% FCS were added to the condensed cells. After this, these cells were put in a 10 cm diameter plate and were placed in a wet 37°C incubator with 5% CO₂.

Afterwards, the cells were washed with phosphate buffered saline (PBS) and placed in a 6 cm diameter Petri dish. Then, 5%

glutaraldehyde fixator was added to the cells for 1 min and then the cells were washed three times by PBS for 5 min. When the Petri dish was dried, the cells ultimately were ready to be tested by AFM.

2.2. AFM nanoindentation: Indentation tests were conducted with a DualScope™ atomic force microscope (DS 95 Series, DME-Danish Micro Engineering, Denmark). Its $x-y$ scan size was $50\ \mu\text{m} \times 50\ \mu\text{m}$ and the resolution was less than 0.1 nm in the z direction and the base height variation ranges were $2.7\ \mu\text{m}$. The probe velocity was $10\ \mu\text{m/s}$ and it was unchangeable. This probe velocity was high compared with the previous studies [18, 19] ($0.125\text{--}5\ \mu\text{m/s}$ and $0.6\ \mu\text{m/s}$) in which the higher probe velocities led to more hysteresis dissipations. The hysteresis was quantified by calculating the area between the indentation and the retraction curves.

Contact mode experimental data were acquired after the cell imaging for each cell. The monolithic silicon pyramidal probe (NanoWorld Pointprobe® CONTR) was used along with a $445\text{--}455\ \mu\text{m}$ length rectangular rod (DualScope™ DS 95 Series, DME-Danish Micro Engineering, Denmark) with spring constants of $0.07\text{--}0.4\ \text{N/m}$ and a pyramid angle of 20° and a tip radius of 10 nm. The spring constant was determined from the thermal vibrations by using the software (DME-SPM Measure & Analysis Software) provided by the manufacturer.

In the nanoindentation procedure, after capturing an image for each cell, three locations were selected along the middle of the longitudinal axis and the force against the indentation curves was obtained (Fig. 1) [19].

2.3. Data analysis: The indentation force (F) was calculated by using Hook's law ($F=kd$), where k and d denote the spring constant and the deflection of the cantilever, respectively. The indentation depth (δ) was calculated from the difference of the AFM cantilever base height and the deflection of the cantilever [18, 19], respectively. Depending on the probe tip shape, there are different forms of the Hertz model [20, 21]. For the pyramidal probe tip, with no adherence, there is a special relation between the force and the indentation depth in an AFM nanoindentation [22]

$$F = kd = \pi E \varphi(\delta) / (1 - \nu^2) \quad (1)$$

$$\varphi(\delta) = \delta^2 \left[\tan(\alpha) / \sqrt{2} \pi \right] \quad (2)$$

in which F is the AFM applied force on a cell, k is the spring constant of the probe, d is the probe deflection, E is the modulus

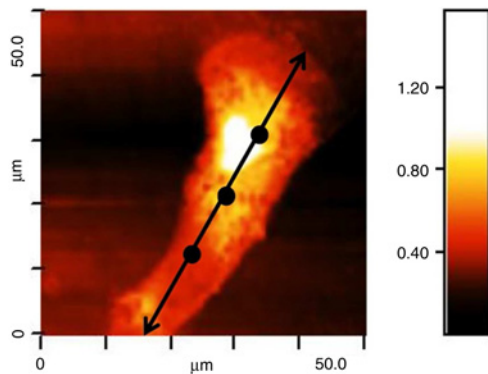


Figure 1 Cardiomyocyte image captured with the atomic force microscope. The bidirectional arrow indicates the middle of the longitudinal axis of this cell approximately and the locations where the measurements are performed are specified.

One of these points was located in the middle of this arrow and two other points were placed near this point approximately with equal distances

of elasticity, ν is the Poisson's ratio, α is the pyramid opening angle, δ is the indentation depth and $\varphi(\delta)$ is a function of the probe geometry, respectively.

The actual geometry of the probe tip is not a sharp pyramid and is described in a better manner as a blunt pyramid with a spherical cap [18]. For the pyramidal probe tip with bluntness, this model relation can be written as:

When $a < b$, the Hertz model relation for the spherical probe tip is used

$$\varphi(\delta) = \delta^{(3/2)} [4R_c^{(1/2)} / 3\pi] \quad (3)$$

in which R_c is the probe tip radius of the curvature. Parameter b is equal to $R_c \cos \alpha$ where the sphere merges tangential with the pyramid faces and a is the contact radius [22].

Note that, when $a < b$, it is the interpretation of a spherical punch of radius R_c and thus $\varphi(\delta)$ is the spherical Hertz model's geometry function.

When $a > b$ [22]

$$\varphi(\delta) = 2/\pi \left(a\delta - \frac{\sqrt{2}a^2}{\pi \tan(\alpha)} \left[\frac{\pi}{2} - \arcsin\left(\frac{b}{a}\right) \right] - \frac{a^3}{3R} + (a^2 - b^2)^{(1/2)} \left[\frac{\sqrt{2}b}{\pi \tan(\alpha)} + \frac{a^2 - b^2}{3R} \right] \right) \quad (4)$$

The contact radius, a , is calculated from the following equation

$$\delta - \frac{a}{\tan(\alpha)} \frac{2^{(3/2)}}{\pi} \left(\frac{\pi}{2} - \arcsin\left(\frac{b}{a}\right) \right) + \frac{a}{R_c} \left[(a^2 - b^2)^{1/2} - a \right] = 0 \quad (5)$$

The contact radii were computed numerically by using an interpolating routine which was written in a computational software (Matlab 7.11, The MathWorks, Inc., Natick, MA, USA).

There are two approaches for the modulus of elasticity calculation. In the first method, an elastic modulus is estimated for the whole nanoindentation data tests [19]. The relation between the force and the elastic modulus can be written as

$$F = \Omega E \quad (6)$$

$$\Omega = \pi \varphi(\delta) / (1 - \nu^2) \quad (7)$$

The elastic modulus was determined by plotting the force as a function of the coefficient Ω and by identifying the resulting slope with the elastic modulus. Another method calculates the elastic modulus for each point particularly by using (1)–(5) [18, 22]. The elastic modulus was calculated by two methods by using the above equations and reported as the mean \pm SD.

In this Letter, a Poisson's ratio of 0.5 was used, which treats the cell as an incompressible material and was suggested for an initial approximation [18].

3. Results

3.1. Adherence: The deflection-indentation depth curves have positive deflection values as the tip retracted from the cell demonstrating that no adherence occurred during the indentation process (Fig. 1).

Furthermore, these curves returned to zero in the retraction phase and it can be concluded that no permanent or plastic deformation remained in these cells after the nanoindentation procedure.

3.2. Hysteresis: The hysteresis or the dissipated energy that appears to be because of the viscous losses was negligible for the cardiomyocyte (Fig. 2); however, the probe scan velocity was high.

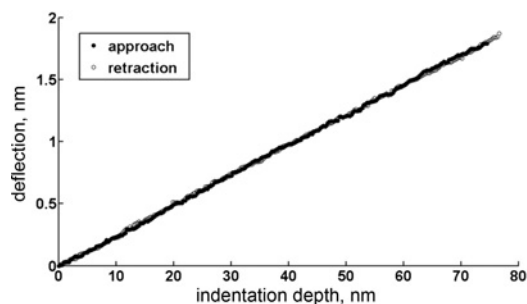


Figure 2 Non-adhesive properties of the cardiomyocyte and it did not show the adherence property

Hence in (1), the total force is equal to the only indentation force and the contact point was assumed to be where the initial probe deflection rises. There are two procedures in the cell AFM test: indentation and retraction. They are not far apart from each other and hence the hysteresis effect was negligible.

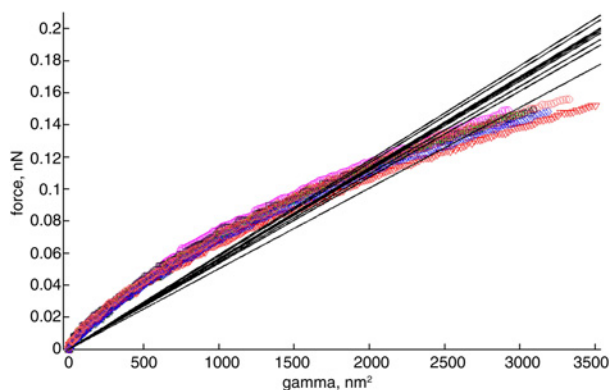


Figure 3 Elastic moduli of the whole cardiomyocytes bodies

It is obvious that the fitting procedure has observable errors and these cells did not behave similar to the linear elastic materials.

3.3. Elasticity calculation: To demonstrate the correlation among the values of the obtained elasticity moduli for the different cells, the graphs of this Section were plotted for all the cell's altogether.

Method 1: From Fig. 3, a line fitting to the experimental data cannot represent the cell's behaviour and it can be concluded from this Figure that the variations of the force as a function of the coefficient (Ω) do not have linear relations and produce considerable fitting errors.

The elastic moduli of the cardiomyocytes was calculated as 55.67 ± 2.56 kPa ($n=9$) on average (Fig. 3).

Method 2: The variation in the elastic moduli with the indentation depth for the cardiac cells is shown in Fig. 4. As illustrated in this Figure, at the higher indentation depths, the elastic modulus approached a constant value, indicating no contributions from the substrate for the indentation depths values in this Letter. Otherwise, with the increasing indentation depth, the elastic modulus would have increased. However, for the indentation depths less than 15 nm most of the variation in the elastic modulus appears to be because of the thermal fluctuations. The consistent variation in the modulus with the different indentation depths indicates that the cardiomyocytes have nonlinear mechanical properties [18].

At 50% of the end of the indentation, the elastic modulus reached the constant values approximately. The elastic moduli at the end of the indentation procedure were 48.08 ± 2.26 kPa ($n=9$) on average (Fig. 4).

3.4. Bluntness effect: To evaluate the effect of the probe tip bluntness on the elastic moduli calculations, elastic modulus-indentation depth curves were collected for the probes with and

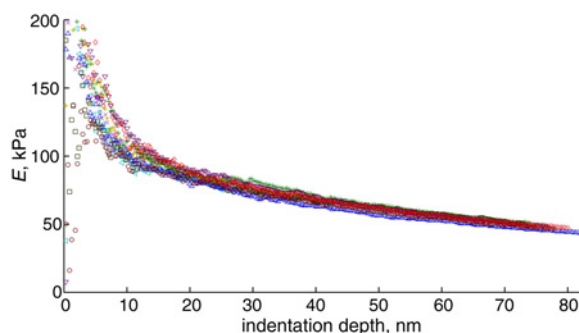


Figure 4 Cardiomyocytes elastic moduli in each indentation depth of the AFM tests

Elastic moduli decreased on increasing the indentation depths and had some nonlinearity.

This mechanical property reached a nearly constant value of more than around 50% of the indentation depths range in the indentation depths.

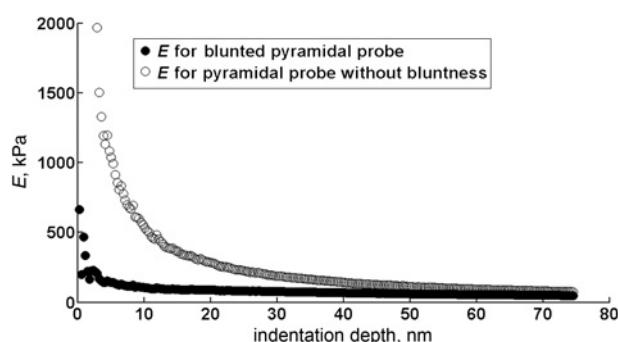


Figure 5 Pyramidal probe tip with and without bluntness

It was observed that assuming the probe tip with bluntness had a good effect on the elastic modulus calculation results and this model predicted the elastic modulus more linearly than the other probe tips without bluntness.

without bluntness (Fig. 5). As illustrated in Fig. 5, the probe tip with bluntness gave more constant elastic moduli values than the pyramidal probe without bluntness. However, the two models collapsed to the same constant values at the higher indentation depths. Hence, it can be concluded that no difference in the two models and no contributions from the substrate existed in this work.

4. Conclusion: In this Letter, the suitability of applying the Hertz model in the cardiomyocytes cell mechanics studies was revealed. The elastic moduli were determined by using two different calculation approaches and the same values were obtained approximately. Also, from these two calculation methods, it was concluded that the cardiomyocytes had nonlinear mechanical properties. Hence, a linear model (such as the Hertz model) cannot evaluate the true mechanical behaviour of these cells. This finding complied with the results of a similar previous paper in which the nonlinear mechanical properties in the myocyte were observed [18].

Furthermore, in the mouse cardiomyocytes, the viscous contribution was negligible and it can be concluded that in this cell, only the elastic properties should be taken into account. It should be noted that even with a high probe z -scan velocity (10 $\mu\text{m/s}$) which led to an augmentation in the viscose dissipations, no hysteresis effects were observed in this cell type [18]. A limitation in this work was the unchangeable probe velocity, therefore the elastic modulus was calculated at the constant probe velocity.

Furthermore, the cell thicknesses were measured with the atomic force microscope and it should be noted that the elastic moduli were obtained for the indentation depths less than 20% of the cell

thickness and were not influenced by the substrate (Fig. 4). The contributions from the substrate had been found to be negligible up to 25% of the thickness of the cell by using the Hertz model and a conical tip [18].

The cardiomyocyte elastic modulus was found to be constant at three positions on the cells along the longitudinal axis around the centre avoiding the boundary effects.

Two mathematical approaches used to calculate the elastic modulus were based on the Hertz model force-indentation depth relation existing in the contact mechanics studies. In the first method, the elastic modulus was determined by plotting an experimental force-gamma coefficient at each indentation depth and by identifying the resulting slope with the modulus of elasticity. In this method, a total modulus was attributed to the cell and it did not depend on the indentation depth. However, the fitting errors were rather high and the correlation coefficients remained between 0.91 and 0.94, demonstrating that the fitted lines deviated extremely from the experimental data. Accordingly, by using this approach, it can be concluded that the mouse myocyte cannot be characterised by the linear elastic behaviour. Hence, the Hertz constitutive model was not suitable for identifying the mechanical properties of this type of cells with this method. In the second method, the elastic modulus was calculated in each point and in each indentation depth. The decrement in the elastic modulus was observed by increasing the indentation depth. At the beginning of the indentation, this decrement occurred vigorously and at the higher indentation depths, a lower decreasing rate was observed. Ultimately, the elastic modulus can be well approximated to be constant at the end of the indentation and was expressed as the elastic modulus of the cell. The value of this elastic modulus was close to the reported value of the previous paper where the rat myocyte had been calculated with this method [19]. The elastic modulus decreased with the increment of the indentation depth as described previously [18], demonstrating an interpretation of the nonlinear behaviour of the mouse cardiac cell.

In the current Letter, the elastic moduli calculated with the first method did not differ from the second method, indicating that determining the elastic modulus did not depend on its method of calculation.

Furthermore, the blunted pyramidal probe model, which more accurately represents the shape of the AFM probe, was less sensitive to the indentation depths than was the pyramidal tip model [18]. However, both the probe geometries gave similar results at the higher indentation depths (indentation depths above 60 nm), when the tip geometry was unimportant and the values of the moduli in both the probe tip models did not differ from each other anymore.

In conclusion, in the mouse cardiac cell study and the determination of the mechanical properties of this cell, the linear elastic assumption for the cell material was not appropriate. On performing the AFM tests and analysing the experimental data, the cardiac cell exhibited nonlinear elastic behaviour. Hence, it can be declared that the Hertz model was not suitable for determining the mechanical properties of the mouse myocyte and this cell's behaviour did not comply with the assumptions of the Hertz model. On the other hand, the viscous dissipation was negligible and it led to the inapplicability of using the viscoelastic models to analyse the cardiomyocyte mechanical properties. Therefore a nonlinear model without the viscose parameters such as the hyperelastic models shall be used for the mechanical characterisation of this cell type.

In a future paper, the mechanical behaviour of the mouse cardiac cell will be determined by applying the hyperelastic models and the suitability of these models will be investigated.

5. Acknowledgments: The authors thank S. H. A. Tafti (speciality heart surgery at the Tehran Heart Center, Tehran, Iran) for invaluable guidance on the subject of the cardiac tissue properties and cells. They also thank the Institute of Nanotechnology and

Tissue Engineering Research Center (Taleghani Hospital, Velenjac, Tehran, Iran) for technical assistance in isolating the cardiac cells and performing the AFM tests. The Iran University of Science and Technology (IUST) is also acknowledged.

6 References

- [1] Kamgoue A., Ohayon J., Usson Y., Riou L., Tracqui P.: 'Quantification of cardiomyocyte contraction based on image correlation analysis', *Cytometry A*, 2009, **75**, pp. 298–308
- [2] Tsamis A., Bothe W., Kvitting J.P., Swanson J.C., Miller D.C., Kuhl E.: 'Active contraction of cardiac muscle: in vivo characterization of mechanical activation sequences in the beating heart', *J. Mech. Behav. Biomed. Mater.*, 2011, **4**, pp. 1167–1176
- [3] Costa K., Holmes J., McCulloch A.: 'Modeling cardiac mechanical properties in three dimensions', *Philos. Trans. R. Soc. Lond. A*, 2001, **359**, pp. 1233–1250
- [4] Nordsletten D.A., Niederer S.A., Nash M.P., Hunter P.J., Smith N.P.: 'Coupling multi-physics models to cardiac mechanics', *Prog. Biophys. Mol. Biol.*, 2011, **104**, pp. 77–88
- [5] Wang V.Y., Lam H.I., Ennis D.B., Cowan B.R., Young A.A., Nash M.P.: 'Modelling passive diastolic mechanics with quantitative MRI of cardiac structure and function', *Med. Image Anal.*, 2009, **13**, pp. 773–784
- [6] Lim C.T., Zhou E.H., Quek S.T.: 'Mechanical models for living cells – a review', *J. Biomech.*, 2006, **39**, pp. 195–216
- [7] Ji B., Bao G.: 'Cell and molecular biomechanics: perspectives and challenges (Citations: 1)', *Ophthalmology*, 2011, **24**, pp. 27–51
- [8] Davidson L., von Dassow M., Zhou J.: 'Multi-scale mechanics from molecules to morphogenesis', *Int. J. Biochem. Cell Biol.*, 2009, **41**, pp. 2147–2162
- [9] Kuznetsova T.G., Starodubtseva M.N., Yegorenkov N.I., Chizhik S. A., Zhdanov R.L.: 'Atomic force microscopy probing of cell elasticity', *Micron*, 2007, **38**, pp. 824–833
- [10] Franz C.M., Puech P.H.: 'Atomic force microscopy – a versatile tool for studying cell morphology, adhesion and mechanics', *Cell Mol. Bioeng.*, 2008, **1**, pp. 289–300
- [11] Webb H.K., Truong V.K., Hasan J., Crawford R.J., Ivanoya E.P.: 'Physico-mechanical characterisation of cells using atomic force microscopy – current research and methodologies', *J. Microbiol. Methods*, 2011, **86**, pp. 131–139
- [12] Zhou Z.L., Ngan A.H., Tang B., Wang A.X.: 'Reliable measurement of elastic modulus of cells by nanoindentation in an atomic force microscope', *J. Mech. Behav. Biomed. Mater.*, 2012, **8**, pp. 134–142
- [13] Li Q.S., Lee G.Y.H., Ong C.N., Lim C.T.: 'AFM indentation study of breast cancer cells', *Biochem. Biophys. Res. Commun.*, 2008, **374**, pp. 609–613
- [14] Kurland N.E., Drira Z., Yadavalli V.K.: 'Measurement of nanomechanical properties of biomolecules using atomic force microscopy', *Micron*, 2012, **43**, pp. 116–128
- [15] Ji B., Bao G.: 'Cell and molecular biomechanics: perspectives and challenges', *Acta Mech. Solida Sin.*, 2011, **24**, pp. 27–51
- [16] King N.M., Methawasin M., Nedrud J., ET AL.: 'Mouse intact cardiac myocyte mechanics: cross-bridge and titin-based stress in unactivated cells', *J. Gen. Physiol.*, 2011, **137**, pp. 81–91
- [17] Tracqui P., Ohayon J., Boudou T.: 'Theoretical analysis of the adaptive contractile behaviour of a single cardiomyocyte cultured on elastic substrates with varying stiffness', *J. Theor. Biol.*, 2008, **255**, pp. 92–105
- [18] Mathur A.B., Collinsworth A.M., Reichert W.M., Kraus W.E., Truskey G.A.: 'Endothelial, cardiac muscle and skeletal muscle exhibit different viscous and elastic properties as determined by atomic force microscopy', *J. Biomech.*, 2001, **34**, pp. 1545–1553
- [19] Lieber S.C., Aubry N., Pain J., Diaz G., Kim S.J., Vatner S.F.: 'Aging increases stiffness of cardiac myocytes measured by atomic force microscopy nanoindentation', *Am. J. Physiol. Heart Circ. Physiol.*, 2004, **287**, pp. 645–651
- [20] Liu K.K., Williams D.R., Briscoe B.J.: 'The large deformation of a single micro-elastomeric sphere', *J. Phys. D, Appl. Phys.*, 1998, **31**, pp. 294–303
- [21] Costa K.D., Yin F.C.: 'Analysis of indentation: implications for measuring mechanical properties with atomic force microscopy', *J. Biomech. Eng.*, 1999, **121**, pp. 462–471
- [22] Rico F., Roca-Cusachs P., Gavara N., Farré R., Rotger M., Navajas D.: 'Probing mechanical properties of living cells by atomic force microscopy with blunted pyramidal cantilever tips', *Phys. Rev. E*, 2005, **72**, pp. 021914